Annihilation of a wedge disclination pair in a hybrid aligned nematic cell

Kiyoshi Minoura,* Yasuyuki Kimura, Kohzo Ito, and Reinosuke Hayakawa
Department of Applied Physics, Graduate School of Engineering, The University of Tokyo, Bunkyo-ku, Tokyo 113, Japan

Toshiaki Miura
National Institute of Materials and Chemical Research, Umezono, Tsukuba 305, Japan

(Received 4 December 1997)

We have investigated the dynamics of the process of annihilation of a wedge disclination pair generated in a nematic cell with hybrid alignment, by quenching it from its isotropic phase. The time evolution of the separation between the defect pair can be classified into two stages: the early stage, with a stringlike pattern of schlieren texture immediately after a defect pair is generated; and the late stage, with a round pattern before the defect pair is annihilated. The experimental results show that the separation between the defect pair decreases linearly with time in the early stage, and then diminishes to zero in proportion to the square root of the time to coalesce the defect pair in the late stage; these are easily explained with a two-dimensional phenomenological model by including an additional field with an ordering effect. By numerical simulation, we have also studied the annihilation dynamics of a three-dimensional equation of motion based on the Frank elastic energy without a phenomenological ordering field. The simulation results are in good agreement with the experimental ones, which indicates that the defect pair behavior in the early stage is attributed to the hybrid alignment, with a coupling energy between the tilt angle and the azimuthal angle. From a comparison between the phenomenological model with the ordering field and the numerical simulation, we can clarify the molecular origin of the ordering field, which has been introduced to explain the unusual annihilation process in the early stage. [S1063-651X(98)12007-X]

PACS number(s): 61.30.Jf, 64.70.Md, 61.30.Gd, 64.60.Ht

I. INTRODUCTION

When a system can undergo a symmetry-breaking phase transition with quenching from a higher symmetry phase to a lower one, various kinds of topological defects, such as walls, point defects, and strings, are generated, depending on the symmetry of the system. Recently, topological defects generated by the breaking of continuous symmetry have been studied experimentally [1–12] and theoretically with the XY model [2–4,13], the Ginzburg-Landau model [9,14–18], and others [10–12,19–23].

In a system quenched from a higher symmetry phase to a lower one and then annealed in the lower symmetry phase, the dynamics of topological defects [24] in the ordering process has attracted the interest of many researchers. The time evolutions of characteristic quantities, such as the number density ρ of defects and the correlation length or separation ξ between defects, are derived from a single time-dependent characteristic length $\lambda(t)$ [19] of the system, which is found to follow the dynamic scaling law in the process of annihilation of defects: $\lambda(t) \sim t^{\phi}$. Here the dynamical scaling exponent ϕ is $\frac{1}{3}$ for a system with a conserved ordering parameter, while ϕ is $\frac{1}{2}$ for the nonconserved system [19]. Many direct observations of defects were carried out on uniaxial nematic liquid crystals, where the symmetry O(3) of the isotropic phase is broken to $D_{\infty h}$ of the nematic phase [25,26]. The time evolutions of ρ and ξ were experimentally studied at a thermal quenching [2–4,9–11] or a pressure jump [11,12], and theoretically discussed, including the computer simulations [2–4,15–22].

Recently, Pargellis *et al.* [2] found a region where the distance D between a largely separated defect pair decreased linearly with time in the smectic-C phase of a thin liquid crystal film, which was contrasted with the other region of D proportional to the square root of time for a smaller separation. The linear time dependence was also reported for a hybrid aligned nematic cell by Lavrentovich and Rozhkov [1]. The string-shaped schlieren texture observed in both cases was quite different from the rounded one in a bulk system. To interpret this result, Pargellis *et al.* [2] phenomenologically assumed an effective ''ordering field'' which aligned a director in the preferential direction through a coupling between the ordering field and the director. As a result, it turned out that the equation of motion, in which a constant line tension of strings (attractive force) and a frictional force were balanced, described well the time evolution of the distance D between a defect pair. However, the molecular origin of the ordering field introduced phenomenologically is still ambiguous.

In this paper, we observe a crossover behavior between the above two regions in a nematic cell with hybrid alignment at a thermal quenching; Lavrentovich and Rozhkov [1] reported only the linear time dependence of D in the whole time range of observation for the same sort of cell. We also apply the dc electric field with various strengths to a nematic sample in the process of annihilation of defect pairs, and investigate the effect of the electric field on the annihilation process. Furthermore, we perform a numerical simulation for this system to examine whether both the static and dynamic behaviors can be explained in terms of the equation of mo-

*Present address: Sharp Company, Kashiwa 277-0005, Japan.

tion based on the three-dimensional Frank elastic energy without the phenomenological ordering field. This treatment is expected to clarify the physical meaning or the molecular origin of the ordering field. The three-dimensional simulation is necessary for describing the annihilation dynamics in a nematic cell with a hybrid alignment.

This paper is organized as follows. In Sec. II, we modify the phenomenological model proposed by Pargellis *et al.* [2], and derive an approximate equation of motion for the interdefect distance D. In Sec. III, the experimental results are presented and analyzed with the modified phenomenological model. In Sec. IV, we discuss the results obtained by the numerical simulation with the equation of motion for director angles on a three-dimensional lattice in the annihilation process.

II. PHENOMENOLOGICAL MODEL

A. Generalized Ginzburg-Landau model

In this paper, we investigate the process of annihilation of a wedge disclination pair with the strengths $s=\pm 1$, which are generated in a sandwich glass cell, forcing hybrid alignment to a nematic liquid crystal: this is planar at the upper surface and subject to no treatment, and homeotropic at the bottom surface and coated with surfactants. We now utilize a phenomenological model proposed by Pargellis *et al.* [2] for a SmC film to describe the annihilation dynamics.

Let the z axis be normal to the glass plates and the molecules be oriented in the xy plane. Then the director field

$$\mathbf{n}(\mathbf{r})=\mathbf{e}_x \sin \Phi(\mathbf{r})+\mathbf{e}_y \cos \Phi(\mathbf{r}), \tag{1}$$

specifies the orientation of molecules in the xy plane, where Φ is the azimuthal angle of molecules as a function of the position $\mathbf{r}$, and $\mathbf{e}_x$ and $\mathbf{e}_y$ are the unit vectors in the x and y directions, respectively. The time evolution of $\mathbf{n}$ can be described by the generalized time-dependent Ginzburg-Landau model as

$$\gamma \frac{\partial \mathbf{n}}{\partial t}=\frac{\delta W}{\delta \mathbf{n}}+\boldsymbol{\eta}, \tag{2}$$

where γ is the damping or friction constant, and η the Gaussian white noise with zero values of mean and moments of higher order than the second. The free energy W is defined by the volume integral

$$W=\int f \, d\mathbf{r} \tag{3}$$

of the free energy density f given by

$$f=\frac{K}{2}(\partial_\alpha n_\beta)^2-\mu \mathbf{N}_0\cdot\mathbf{n}-\frac{\Delta\varepsilon}{2}(\mathbf{E}\cdot\mathbf{n})^2 \tag{4}$$

where N_0 is the direction vector of the ordering field proposed phenomenologically by Pagellis *et al.* [2], K the elastic constant, μ the coupling constant between $\mathbf{N}_0$ and $\mathbf{n}$, $\Delta\varepsilon$ the dielectric anisotropy, and $\mathbf{E}$ the external electric field. The first term on the right-hand side of Eq. (4) represents the usual Frank elastic energy in the one-constant approximation; the second term is the energy aligning the director field $\mathbf{n}$ to the direction of the ordering field $\mathbf{N}_0$, similarly to the energy of the dipole moment in a uniform electric field; and the third term a coupling energy between $\mathbf{n}$ and the external electric field $\mathbf{E}$ through a quadrupolar interaction. By choosing both directions of the ordering field $\mathbf{N}_0$ and the electric field $\mathbf{E}$ to be parallel to the y axis, and by substituting Eq. (1) into Eq. (4), we can rewrite the free energy density f as

$$f=\frac{K}{2}(\boldsymbol{\nabla}\Phi)^2+\mu N_0(1-\cos\Phi)+\frac{\Delta\varepsilon E^2}{2}\sin^2\Phi. \tag{5}$$

The substitution of Eqs. (1) and (3) by Eq. (5) into Eq. (2) yields the equation of motion for Φ as

$$\gamma\frac{\partial\Phi}{\partial t}=K\nabla^2\Phi-\mu N_0 \sin\Phi-\frac{\Delta\varepsilon}{2}E^2\sin 2\Phi. \tag{6}$$

To clarify the process of annihilation of the defect pair, we treat some limiting cases in Secs. II B and II C, where we reduce Eq. (6) to a simpler equation of motion for the distance D between a defect pair.

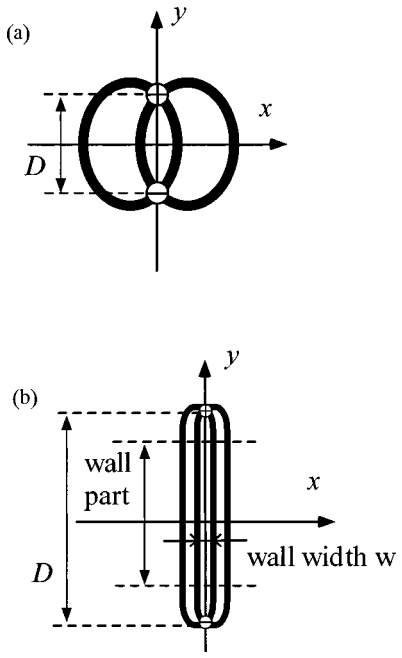

FIG. 1. Schematic pictures (a) and (b) of schlieren textures to be observed between crossed polarizers of optical microscope in late and early stages, respectively. The wall width w is defined as an interval of black brushes in (b). We call the part where the director field $\boldsymbol{n}$ depends only on the x coordinate the ''wall part.''

B. Without the ordering field or the external electric field ($N_0=E=0$)

First we consider the case where no ordering or external electric field exists, and thus we have only to consider the Frank elastic energy. When the defects with the strengths $s=\pm 1$ are placed at the positions $(0,\pm D/2)$, respectively, the schlieren texture observed between crossed polarizers is round shaped, as shown in Fig. 1(a). By using Eqs. (3) and (5), one can obtain the attractive force $F_a=\partial W/\partial D=2\pi K/D$ between the defect pair [24]. It is natural that the attractive force is similar to the Coulombic one in the two-

dimensional space, because the time-independent equation obtained from Eq. (6) with $N_0=E=0$ is reduced to the Laplace equation. On the other hand, the frictional force $F_\mu \equiv \gamma \partial D/\partial t$ depends logarithmically on the defect size R, which is evaluated to be nearly equal to the separation D in the present case [2]. Balancing F_μ with F_a, one can obtain the equation describing the coalescence of a pair of ± 1 disclinations as [2]

$$\pi\gamma \ln\left(\frac{D}{R_c}\right)\frac{\partial D}{\partial t}=-\frac{2\pi K}{D}, \tag{7}$$

where R_c is a core radius [24]. The solution of Eq. (7) is given by

$$D^2\left(\ln\frac{D}{R_c}-\frac{1}{2}\right)=\frac{4K}{\gamma}(t_0-t), \tag{8}$$

where t_0 is the time of the coalescence ($D=0$). When one observes defects with an optical microscope, D is much larger than R_c, which is typically several nanometers [24] for thermotropic liquid crystals. Consequently, $\ln(D/R_c)$ is weakly dependent on D, and hence it is seen from Eq. (8) that $D\propto(t_0-t)^{1/2}$, that is, D diminishes in proportion to the square root of the time to coalesce the defect pair.

C. With the ordering field and without the external electric field ($N_0\neq 0$, $E=0$)

We now consider the case where the ordering field is dominant over the elastic energy and no external electric field exists. In this case, it is expected that the pattern of the defect pair is a string-shaped schlieren texture with a wall part [Fig. 1(b)], since the ordering field forces molecules to orient toward the ordering direction N_0. That is, the orientation of the directors depends almost exclusively on x. Thus, by neglecting the y dependence of Φ, we obtain a time-independent solution of Eq. (6) under the boundary conditions $\partial\Phi/\partial x=0$ and $\Phi=2\pi$ at $x\to\infty$ as

$$\Phi=4\tan^{-1}\left[\exp\left(\frac{x-x_0}{w}\right)\right], \tag{9}$$

where x_0 is an integration constant, and w is the width of a disclination wall defined by the distance for a phase change from $\pi/2$ to $3\pi/2$:

$$w=\sqrt{K/\mu N_0}. \tag{10}$$

With the angular distribution of directors given by Eq. (9), the schlieren texture at the wall part, observed between crossed polarizers, would be slender, as shown in Fig. 1(b). This pattern is realized only when the length of the disclination wall or D is much larger than the width w. When D becomes of the same order as w, the elastic energy dominates over the energy due to the ordering field, and hence the defect pair behavior exhibits a crossover to the coalescence process in the absence of ordering field. Similar to Sec. II B, one has the equation of motion [2]

$$\pi\gamma \ln\left(\frac{w}{R_c}\right)\frac{\partial D}{\partial t}=-\frac{8K}{w}. \tag{11}$$

The left- and right-hand sides of Eq. (11) represent the frictional and attractive forces, respectively. Thus, the disclination pair approach to each other as

$$D=\frac{8K}{\pi\gamma w\,\ln(w/R_c)}(t_0-t); \tag{12}$$

that is, D decreases linearly with the time to the coalescence of the pair.

D. With both the ordering field and the external electric field ($N_0\neq 0$, $E\neq 0$)

Next we discuss the effect of the external dc electric field on the wall width w and on the time evolution of the annihilation process. The dc electric field also has an ordering effect, so that the pattern observed with an optical microscope is expected to be string shaped with a wall part. By the same approximation as in Sec. II C, the time-independent solution of Eq. (6) at the wall part is given by

$$\Phi=\cos^{-1}\left[\frac{(p-4)(1+e^{2t})-2(3p-4)e^t}{(p-4)(1+e^{2t})+2(p+4)e^t}\right], \tag{13}$$

where $p=(4\mu N_0/\Delta\varepsilon E^2)+4$ and $t=\sqrt{4\mu N_0/K}(x-x_0)$. From Eq. (13), the wall width w is obtained as

$$w=w(E)=\left(\frac{K}{4\mu N_0+4\Delta\varepsilon E^2}\right)^{1/2}\ln\left\{3+\frac{2\Delta\varepsilon E^2}{\mu N_0}+\left[\left(4+\frac{2\Delta\varepsilon E^2}{\mu N_0}\right)\left(2+\frac{2\Delta\varepsilon E^2}{\mu N_0}\right)\right]^{1/2}\right\}. \tag{14}$$

In this case, the attractive force $F_a=\partial W/\partial D$ is given by

$$F_a=F_a(E)=4\sqrt{K}\left(\sqrt{\mu N_0+\Delta\varepsilon E^2}+\frac{\mu N_0}{\sqrt{\Delta\varepsilon E^2}}\ln\frac{\sqrt{\mu N_0+\Delta\varepsilon E^2}+\sqrt{\Delta\varepsilon E^2}}{\sqrt{\mu N_0}}\right). \tag{15}$$

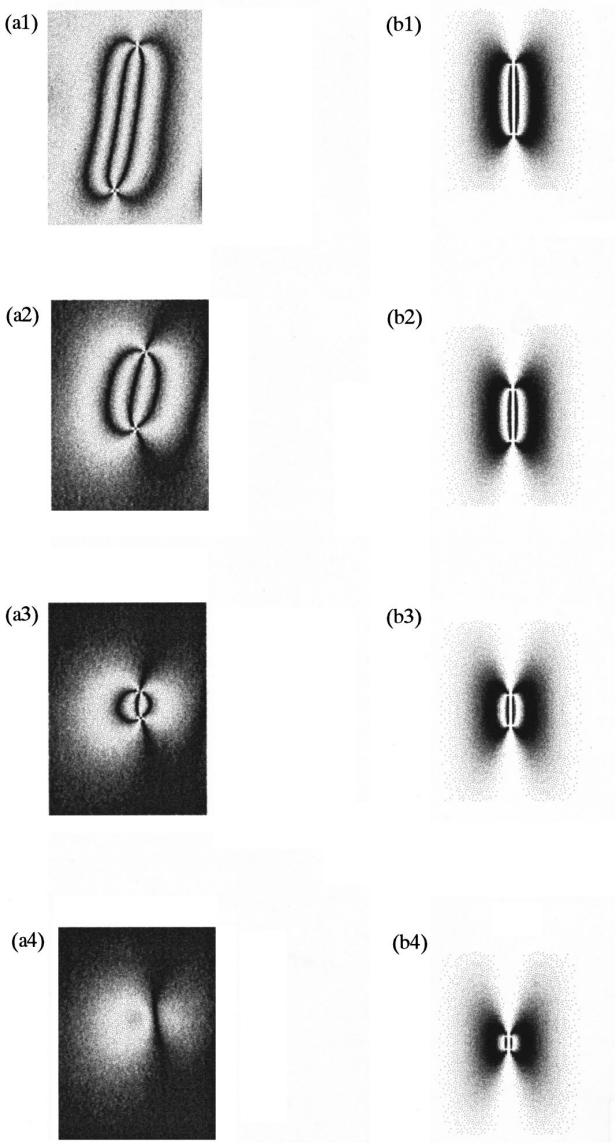

FIG. 2. The pictures of annihilation of a disclination pair with the strength $s=\pm 1$ in a hybrid aligned nematic cell, observed as schlieren textures between crossed polarizers of an optical microscope: (a) experiment and (b) simulation. As for the experimental result, the time to coalesce and the initial separation of the defects are of the order of 100 s and 100 μm, respectively.

On the other hand, the frictional force F_μ can be obtained by substituting Eq. (14) into the left-hand side of Eq. (11). The balance between F_a and F_μ yields the time dependence of D as

$$D=\frac{F_a(E)}{\pi\gamma \ln[w(E)/R_c]}(t_0-t). \tag{16}$$

The interdefect distance D decreases linearly with the time to coalesce, which is similar to the case of a strong ordering field without the external electric field, as described in Sec. II C.

III. EXPERIMENTAL RESULTS AND DISCUSSION

The nematic liquid crystal 4-cyano-4′-*n*-pentylbiphenyl (5CB) was sandwiched between two glass plates. One of the

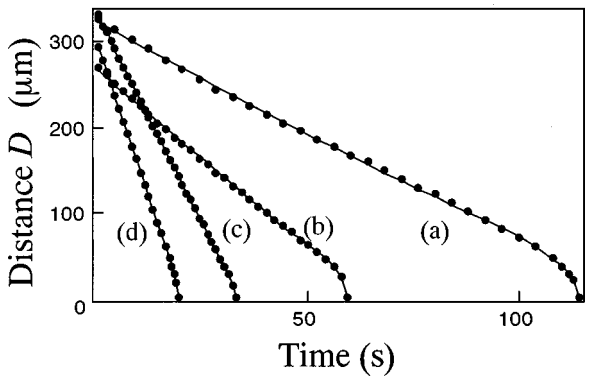

FIG. 3. The time dependence of the distance D between a defect pair under dc electric fields of (a) 0, (b) 2, (c) 6, and (d) 10 kV/m. Note that D decreases linearly with time in the early stage, and then in proportion to the square root of the time, to coalesce the defect pair in the late stage. The annihilation velocity of the defect pair in the early stage increases with increasing dc electric field.

cell surfaces was coated with homeotropic alignment material such as surfine-150 (Dainippon Ink and Chemicals, Inc.) and the other was kept clean with no treatment. Aluminum foil 15 μm thick was used as a spacer and an electrode for applying the dc electric field parallel to the glass plates. In addition, polyethylenetelephthalate and polytetrafluoroethylene (teflon) films were used for adjusting the cell thickness to various values (5.5, 11, 30, and 65 μm). The sample cell was temperature controlled within an accuracy of 50 mK, and was observed with a polarizing microscope. The image of disclination pair was recorded on a video tape through a CCD camera mounted on the microscope. The observation was performed by quenching the liquid crystal sample from the isotropic phase at a temperature a little higher than the transition point (35.3 °C) to the nematic phase at a temperature about 0.2 °C below the transition point, and then keeping it at this temperature (35.1 °C).

When the sample was quenched, many wedge disclination pairs with strengths of ± 1 were generated, and gradually disappeared in pairs. The disclination pairs exhibited a schlieren texture with four white and black brushes under the polarizing microscope. Some pictures of schlieren pattern in the annihilation process are shown in Fig. 2(a). The typical time dependence of the separation D between a disclination pair is shown in Fig. 3(a). The annihilation process is found to be roughly divided into two time regions with different time dependences of D. In the early stage where D is large, D decreases linearly with time, and the defect pair is connected with string-shaped walls. In contrast, in the late stage where D is small, D decreases in proportion to the square root of the time to coalesce the defect pair. These behaviors are in good agreement with the theoretical results obtained from the two-dimensional phenomenological model in Sec. II.

Moreover, we applied the dc electric field parallel to the cell surfaces as a controllable or external ''ordering field'' in order to evaluate the elastic constant K and to observe any change in the annihilation process due to the external electric field. The time dependence of D under various values of dc electric field is shown in Figs. 3(b), 3(c), and 3(d). We see the crossover time between the two stages shifts to a later

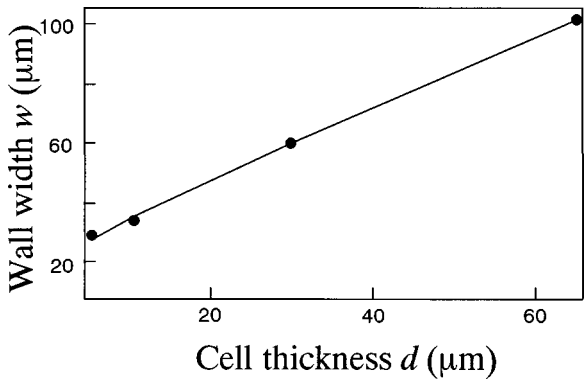

FIG. 4. Experimental result for the dependence of the wall width w on the cell thickness d. Note that w increases with increasing d.

one, and the duration of the late stage becomes shorter as the strength of dc electric field increases. It is also found that the applied dc electric field accelerates the annihilation of disclination pair in the early stage, which indicates that the dc field reinforces the intrinsic ordering field. These results are qualitatively explainable by the phenomenological model treated in Sec. II.

We also measured the wall width w for various values of cell thickness and dc electric field. The results are plotted in Figs. 4 and 5. The solid curve in Fig. 5 is the best-fitted one by using Eq. (14) with fitting parameters of $\mu N_0/K = 4.11 \times 10^8$ m^{-2} and $\Delta\varepsilon/4K = 11.1$ V^{-2}. With this value of $\Delta\varepsilon/4K$ and $\Delta\varepsilon = 9.74 \times 10^{-11}$ N/V^2 [26], the elastic constant K is evaluated as 2.0×10^{-12} N, which is somewhat smaller than that in the bulk, 1.0×10^{-11} N [26]. This discrepancy may be ascribed to the difference in dimensionality. In this analysis, all of the variables are defined in the two-dimensional space, while the experiment was carried out in a real three-dimensional space. In Sec. IV, we will make a numerical simulation in the three-dimensional space.

IV. RESULTS AND DISCUSSION FOR NUMERICAL SIMULATION

To investigate the time evolution of annihilation process, we perform a numerical simulation by introducing the three-dimensional Frank elastic energy and the anchoring energy without the phenomenological ordering field, and compare the results with those obtained by the two-dimensional phenomenological theory as described in Sec. II.

The three-dimensional director field is expressed as

$$\boldsymbol{n}[\Phi(\boldsymbol{r}),\Theta(\boldsymbol{r})] = (\sin\Phi(\boldsymbol{r})\sin\Theta(\boldsymbol{r}), \cos\Phi(\boldsymbol{r})\sin\Theta(\boldsymbol{r}), \cos\Theta(\boldsymbol{r})), \tag{17}$$

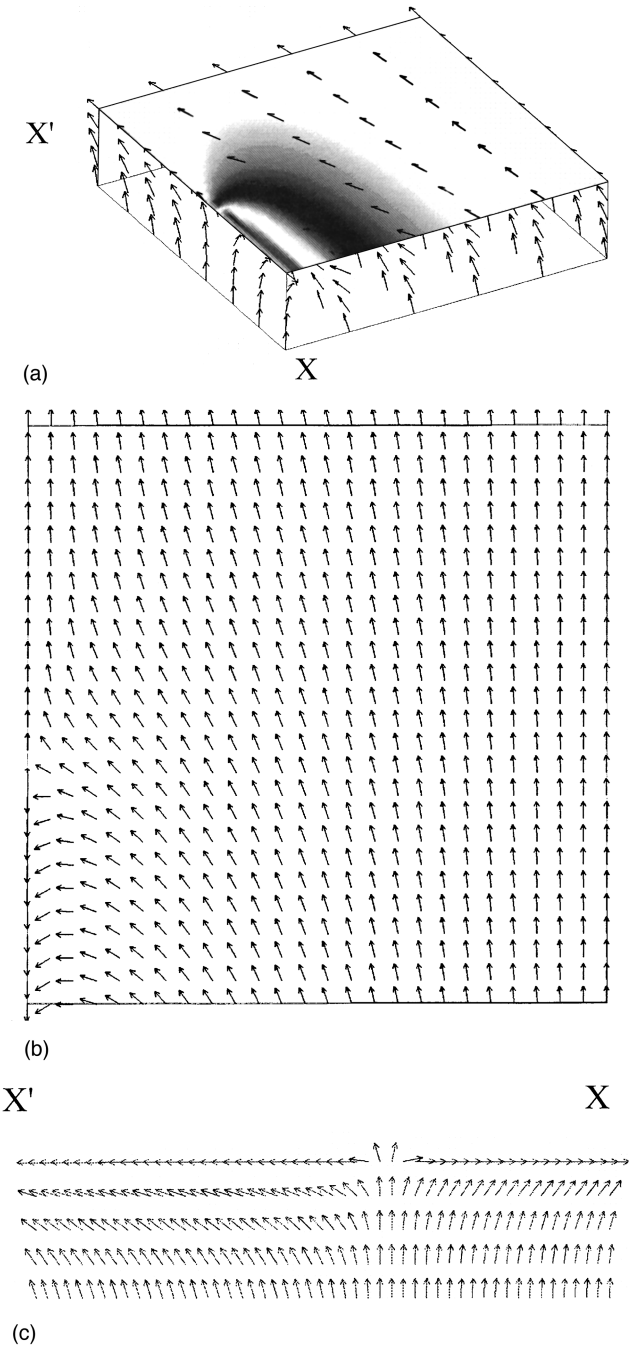

FIG. 6. The three-dimensional vector picture of initial configurations for a numerical simulation in the hybrid alignment, which is divided into a quarter piece. An image of schlieren textures under a polarizing microscope is attached on the top surface. Two-dimensional vector pictures of the top surface and the vertical cross section ($X-X'$) are shown in (b) and (c), respectively.

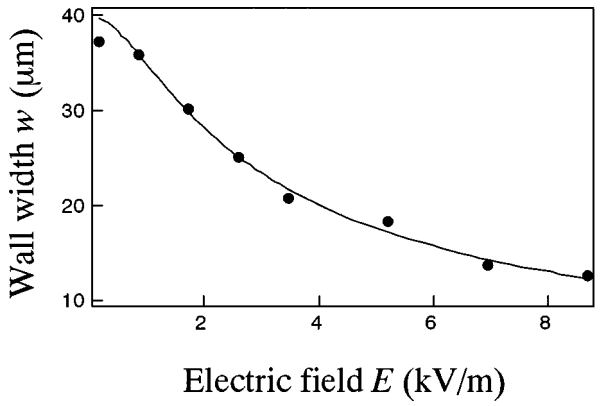

FIG. 5. Experimental result for the dependence of the wall width w on the dc electric field E. Note that w decreases with increasing E.

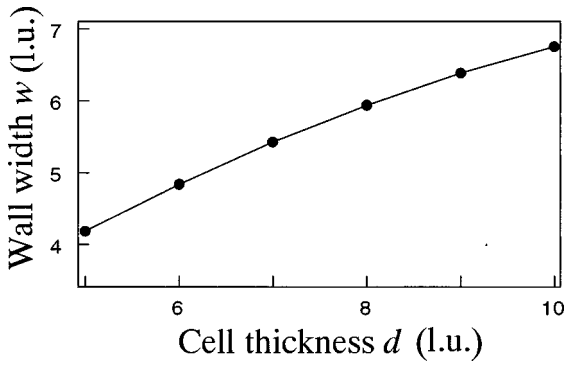

FIG. 7. Simulation result for the dependence of the wall width w on the cell thickness d in lattice units (l.u.'s). This is in good agreement with the experimental result shown in Fig. 4.

where Φ is the azimuthal angle and Θ is the tilt angle. The free energy W is defined as [1]

$$W=\int dv f_F+\int dS f_S, \tag{18}$$

$$\begin{aligned} f_F=\frac{K}{2}[&(\nabla\Theta)^2+\sin^2\Theta\{(\nabla\Phi)^2+(\Phi_y\sin\Phi \\ &-\Phi_x\cos\Phi)\Theta_z+(\Theta_x\cos\Phi-\Theta_y\sin\Phi)\Phi_z\} \\ &+\sin\Theta\cos\Theta(\Theta_y\Phi_x-\Phi_y\Theta_x)] \\ &+\frac{\Delta\varepsilon}{2}E^2\sin^2\Phi\sin^2\Theta, \end{aligned} \tag{19}$$

$$\begin{aligned} f_S=&(K_{13}\cos^2\Theta+K_{24})(\Theta_x\sin\Phi+\Theta_y\cos\Phi) \\ &-K_{13}\Theta_z\sin\Theta\cos\Theta \\ &+(K_{13}+K_{24})\sin\Theta\cos\Theta(\Phi_x\cos\Phi-\Phi_y\sin\Phi) \\ &+\sum_{i=1,2}\frac{W_A}{2}\sin^2(\Theta-\alpha_i). \end{aligned} \tag{20}$$

Here f_F is the ordinary Frank elastic energy density in the one-constant (K) approximation, f_S is the quasisurface contribution of the Frank elastic energy with mixed splay-bend (K_{13}) and saddle-splay (K_{24}) elastic constants, W_A is the anchoring energy in the Θ direction, and the subscripts x, y, and z mean partial differentiation. By substituting the free energy W into Eq. (2), we obtain a pair of equations of motion

$$\gamma\sin^2\Theta\frac{\partial\Phi}{\partial t}=-\frac{\partial W}{\partial\Phi}, \tag{21}$$

$$\gamma\frac{\partial\Theta}{\partial t}=-\frac{\partial W}{\partial\Theta}. \tag{22}$$

We performed a numerical simulation with these master equations converted by the finite differential method. The time evolution was pursued using a $101\times101\times5$ array of lattice points, and for calculating the dependence on the cell thickness d we used six arrays: $101\times101\times5$, 6, 7, 8, 9, and 10. One example of initial configurations is shown in Fig. 6.

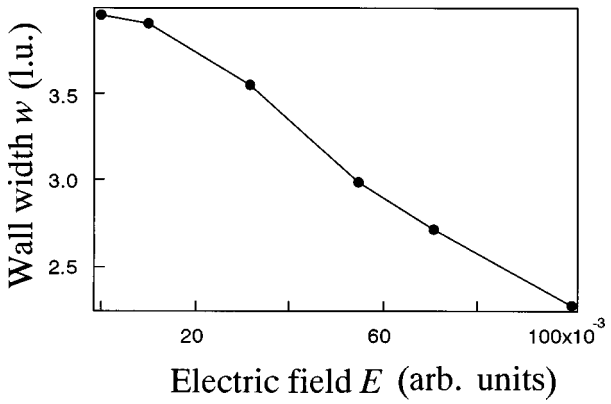

FIG. 8. Simulation result for the dependence of the wall width w on the dc electric field E. This is in good agreement with the experimental result shown in Fig. 5.

All the runs were performed on a work station (Hewlett Packard C110). We set the conversion coefficient Δt from a calculation step to real time, and the conversion coefficient Δd from a lattice unit to real spacing, so that the condition $K\Delta t/\gamma\Delta d^2=0.1$ was satisfied. This condition implies that Δt is sufficiently small against Δd^2, which assures that the diffusion process is realized. In this simulation, we ignored the elastic constants K_{13} and K_{24}, which were expected to be much smaller than the strong anchoring energy W_A. First we calculated an initial configuration of directors by using Eqs. (21) and (22) without time-dependent terms, and adopting the free boundary condition at the lattice edge. This procedure is equivalent to determining the configuration with the smallest deformation energy by holding a defect pair still. Figures 7 and 8 show the numerical simulation results for the dependences of the wall width w on the cell thickness d and the external dc electric field E, respectively. These results are in good agreement with the experimental ones shown in Figs. 3 and 4.

Next we simulated step by step the time evolution of Φ and Θ in the annihilation process by using Eqs. (21) and (22) with the time-dependent terms under the free boundary condition at the lattice edge. The time dependence of D obtained from the numerical simulation is shown in Fig. 9, which is in a good agreement with Fig. 3 for the experimental results. Simulated schlieren patterns in the annihilation process are

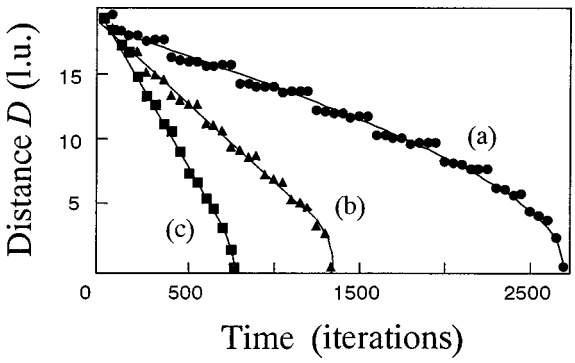

FIG. 9. Simulation results for the time dependence of the distance D between a defect pair under various dc electric fields of (a) 0, (b) 1×10^{-3}, and (c) 5×10^{-3} (arbitrary units). These are in good agreement with the experimental results shown in Fig. 3.

shown in Fig. 2(b), and also agree well with the experimental ones in Fig. 2(a).

The above results indicate that the present system is described by both the two-dimensional model with the phenomenological ordering field and the three-dimensional model without the ordering field. Since the physical meaning of all the terms involved in the three-dimensional model is clear, the comparison of the corresponding terms in the two models can clarify the molecular origin of the ordering field in the two-dimensional model. Thus it is found that the ordering field μN_0 in Eq. (5) corresponds to $(\Theta_z\Phi_x - \Phi_z\Theta_x)\sin^2\Theta$ in Eq. (19). In the present system, where no twist deformation is forced by the glass plates and 5CB has no chirality, Φ_z is nearly equal to zero. Further, the anchoring force for the tilt angle is so strong that Θ_x is also nearly equal to zero. Then the ordering field μN_0 mainly arises from the term $\Theta_z\Phi_x \sin^2\Theta$; that is, μN_0 is approximately proportional to Θ_z. Since liquid crystal molecules are forced to align homeotropically at the bottom surface of the cell and to align in a planar manner at the upper surface, the value of Θ_z is roughly estimated to be $\pi/(2d)$, where d is the cell thickness. Hence it is expected that the ordering field, which is approximately proportional to Θ_z, decreases with increasing d. On the other hand, according to Eq. (10), the ordering field is inversely proportional to the square of the wall width w. From these relations it turns out that the thicker the cell thickness d is, the wider the wall width w is, which is in good agreement with the experimental results as shown in Fig. 4. This supports the correspondence between the ordering field μN_0 in the two-dimensional model and the term $(\Theta_z\Phi_x - \Phi_z\Theta_x)\sin^2\Theta$ in the three-dimensional one; that is, the ordering field arises from a coupling energy between deformations of the tilt angle Θ and of the azimuthal angle Φ. In other words, the molecular origin of the ordering field in the present system is the hybrid alignment which produces nonzero Θ_z.

Another possible origin of the ordering field may be the quasisurface contribution f_s of the Frank elastic energy with the elastic constants K_{13} and K_{24}. This contribution has been neglected in the discussion so far, because the contribution is considered to be much less than that of the bulk. It was recently reported, however, that K_{13} and K_{24} are of the same order of magnitude as the elastic constants in the bulk [25]. Our simulation results suggest a possibility that f_s may play an important role under sufficiently weak anchoring. This point still remains to be studied.

V. CONCLUSION

We experimentally observed the crossover behavior from an early stage to a late one in the process of annihilation of wedge disclination pair in the hybrid aligned nematic cell. It was found that a two-dimensional analysis with a phenomenological ordering field explained the early stage well. The dc electric field also had an ordering effect similar to the phenomenological ordering field. To clarify the molecular origin of the ordering field, we performed the three-dimensional numerical simulation. The results showed that the ordering field corresponded to the coupling energy between the deformations of tilt angle and azimuthal angle, and that the origin of the ordering force in this case was the hybrid alignment of liquid crystal molecules.

[1] O. D. Lavrentovich and S. S. Rozhkov, Pis'ma Zh. Eksp. Teor. Fiz. **47**, 210 (1988) [JETP Lett. **47**, 254 (1988)].

[2] A. N. Pargellis, P. Finn, J. W. Goodby, P. Panizza, B. Yurke, and P. E. Cladis, Phys. Rev. A **46**, 7765 (1992).

[3] A. N. Pargellis, S. Green, and B. Yurke, Phys. Rev. E **49**, 4250 (1994).

[4] B. Yurke, A. N. Pargellis, T. Kovacs, and D. A. Huse, Phys. Rev. E **47**, 1525 (1993).

[5] C. D. Muzny and N. A. Clark, Phys. Rev. Lett. **68**, 804 (1992).

[6] T. Nagaya, H. Hotta, H. Orihara, and Y. Ishibashi, J. Phys. Soc. Jpn. **60**, 1572 (1991).

[7] J. Pang, C. D. Muzny, and N. A. Clark, Phys. Rev. Lett. **69**, 2783 (1992).

[8] T. Nagaya, H. Orihara, and Y. Ishibashi, J. Phys. Soc. Jpn. **56**, 3086 (1987).

[9] B. Yurke, A. N. Pargellis, I. Chuang, and N. Turok, Physica B **178**, 56 (1992).

[10] H. Orihara and Y. Ishibashi, J. Phys. Soc. Jpn. **55**, 2151 (1986).

[11] A. Pargellis, N. Turok, and B. Yurke, Phys. Rev. Lett. **67**, 1570 (1991).

[12] I. Chuang, N. Turok, and B. Yurke, Phys. Rev. Lett. **66**, 2472 (1991).

[13] J. Toner and Y. Tu, Phys. Rev. Lett. **75**, 4326 (1995).

[14] H. Pleiner, Phys. Rev. A **37**, 3986 (1988).

[15] H. Toyoki and K. Honda, Prog. Theor. Phys. **78**, 237 (1987).

[16] H. Toyoki, Phys. Rev. A **42**, 911 (1990).

[17] H. Nishimori and T. Nukii, J. Phys. Soc. Jpn **58**, 563 (1988).

[18] H. Toyoki, J. Phys. Soc. Jpn. **63**, 4446 (1994).

[19] M. Mondello and N. Goldenfeld, Phys. Rev. A **42**, 5865 (1990).

[20] B. Kim, S. J. Lee, and J. R. Lee, Phys. Rev. E **53**, 6061 (1996).

[21] G. Ryskin and M. Kremenetsky, Phys. Rev. Lett. **67**, 1574 (1991).

[22] G. Huber and P. Alstrøm, Physica A **195**, 448 (1993).

[23] I. Chuang, R. Durrer, N. Turok, and B. Yurke, Science **251**, 1336 (1991).

[24] P. G. deGennes, *The Physics of Liquid Crystals* (Oxford University Press, London, 1974).

[25] O. D. Lavrentovich and V. M. Pergamenshchik, Int. J. Mod. Phys. B **9**, 251 (1995).

[26] The 142nd committee of JCPS for organic materials in information, division of liquid crystal: *Encyclopedic Dictionary of Liquid Crystals* (Baifukan, Tokyo, 1989).